RSC Advances

PAPER

View Article Online
View Journal | View Issue

Cite this: *RSC Adv.*, 2021, **11**, 11192

Modulation of amyloid fibrillation of bovine β-lactoglobulin by selective methionine oxidation†

Sanhita Maity,[a] Nayim Sepay,[a] Sampa Pal,[a] Subrata Sardar,[a] Hasan Parvej,[a] Swarnali Pal,[a] Jishnu Chakraborty,[b] Anirban Pradhan[c] and Umesh Chandra Halder*[a]

Deposition of oxidation-modified proteins during normal aging and oxidative stress are directly associated with systemic amyloidoses. Methionine (Met) is believed to be one of the most readily oxidisable amino acid residues of protein. Bovine beta-lactoglobulin (β-lg), a model globular whey protein, has been presented as a subsequent paradigm for studies on protein aggregation and amyloid formation. Herein, we investigated the effect of *t*-butyl hydroperoxide (*t*BHP)-induced oxidation on structure, compactness and fibrillation propensity of β-lg at physiological pH. Notably, whey protein modification, specifically Met residues, plays an important role in the dairy industry during milk processing and lowering nutritional value and ultimately affecting their technological properties. Several bio-physical studies revealed enhanced structural flexibility and aggregation propensity of oxidised β-lg in a temperature dependent manner. A molecular docking study is used to predict possible interactions with *t*BHP and infers selective oxidation of methionine residues at 7, 24 and 107 positions. From our studies, it can be corroborated that specific orientations of Met residues directs the formation of a partially unfolded state susceptible to fibrillation with possible different cytotoxic effects. Our studies have greater implications in deciphering the underlying mechanism of different whey proteins encountering oxidative stress. Our findings are also important to elucidate the understanding of oxidation induced amyloid fibrillation of protein which may constitute a new route to pave the way for a modulatory role of oxidatively stressed proteins in neurological disorders.

Received 23rd October 2020
Accepted 5th March 2021

DOI: 10.1039/d0ra09060c

rsc.li/rsc-advances

Introduction

Oxidative damage is considered as a likely cause of age-related brain dysfunction because the brain is believed to be particularly vulnerable to oxidative stress due to a relatively high rate of oxygen free radical generation without commensurate levels of anti-oxidative defenses.[1] In particular, one category of disease in which oxidative damage is found extensively is neurodegenerative diseases including Alzheimer's (AD), Huntington's (HD), Parkinson's diseases (PD), and prion diseases.[2–6] In particular, post-mortem analysis of the AD brain has shown elevated levels of protein oxidation, lipid peroxidation, and oxidative damage to mitochondria.[7,8] Specifically, protein oxidation involved covalent cross-linkages, fragmentation of covalent bonds, and modification of amino acids including methionine, cysteine, histidine, tryptophan, and tyrosine.[9] Methionine (Met) is one of the most oxidation-prone amino acid and is converted to methionine sulfoxide or sulfone derivatives by different mechanisms, such as hydrogen peroxide treatment, metal catalyzed reactions, and UV exposure.[10]

Recently, most research work has been focused on the inhibition of fibril formation by the employment of small molecules. These potent modulators are believed to stabilize the monomer by blocking the formation of toxic oligomers and divert the monomeric protein to off-pathway non-toxic intermediates. Small molecules agents are being developed to inhibit aggregation of Aβ,[12] α-synuclein[13] and prions.[14]

It has been demonstrated that oxidation of the susceptible Met residues of proteins has been shown to result in structural changes,[11,12] decreased stability,[13,14] increased propensity to aggregation[15] and loss of biological functions. It is worth mentioning that even subtle modifications at single residue level in protein structures may reorganize specific inter-protein and protein-solvent interactions. In addition, methionine oxidation serves as a common modulator of fibril formation and has been shown to suppress the aggregation of β-amyloid peptide, prion protein (PrP), transthyretin, apolipoprotein C-II α-synuclein and human serum albumin.[16–21] Interestingly, in

[a]*Department of Chemistry, Jadavpur University, Kolkata 700032, India. E-mail: uhalder2002@yahoo.com*

[b]*Department of Chemistry, Camellia Institute of Engineering and Technology, Budbud, Burdwan, WB, India*

[c]*Department of Chemistry, Ramakrishna Mission Residential College (Autonomous), Vivekananda Centre for Research, Narendrapur, Kolkata-700103, India*

† Electronic supplementary information (ESI) available. See DOI: 10.1039/d0ra09060c

some cases the opposite tendency was observed for k-casein and apolipoprotein A-I.[22,23] Despite the conflicting reports, the susceptibility or aggressiveness of several amyloid diseases is significantly affected by the presence of a methionine residue in the primary sequence of the protein.

Bovine beta-lactoglobulin (β-lg), a well-known globular whey protein in ruminant milk (MW = 18.3 kDa), has been presented as a subsequent paradigm for studies on protein aggregation and amyloid formation.[24] Bovine β-lg belongs to a class of effective carrier protein of oxidation-sensitive hydrophobic drugs and nutraceuticals, having a unique acidic pH resistivity and potential encapsulating property.[13] At elevated temperature (above 50 °C), the protein undergoes a conformational change, with exposure of buried hydrophobic groups and the thiol (–SH) group (Cys121). However, the protein β-lg is believed to form amyloid fibrils when heated above 75 °Cat physiological pH with all characteristic features observed in many amyloid diseases.[25,26] The chemical modifications of β-lg is studied in attempt to broaden its application in food and pharmaceutical industry by improving its techno-functional properties, as well as to increase its digestibility and reduce its allergenic potential.[27] The most oxidation-sensitive amino acids in this protein are the four methionine residues located at 7, 24, 107 and 145 positions.[28] In biological systems, the reaction that yields methionine sulfone is less common than that which yields methionine sulfoxide.[10] In this context, it appears crucial to emphasize that modulation of protein aggregation pathway may be guided by selective methionine oxidation.

Herein, we investigate the effect of *t*BHP-induced methionine oxidation on structure and function of β-lg. *t*BHP was found to be a selective methionine-specific oxidant, capable of oxidizing surface exposed and partially buried methionine residues to sulfoxide form stoichiometrically.[29] We demonstrate that, in our experimental conditions, the oxidation of methionine residues of β-lg modifies the fibril formation propensity, modulates the route of amyloid fibrillation and morphologies of the final aggregates.

Experimental

Materials and methods

Bovine beta lactoglobulin (β-lg) was purified from cow milk as described in the previous report.[30] The final product was lyophilized and stored at 4 °C for further use. Sodium dihydrogen phosphate was purchased from Merck (Mumbai, India). Different fluorescent probes, *viz.*, 8-anilinonaphthalene-1-sulfonic acid ammonium salt (ANS), Thioflavin T (Th T) were purchased from Sigma Chemical Co. (St. Louis, USA). *tert*-Butylhydroperoxide (*t*BHP) (70% in water) was obtained from Spectrochem, India. The other chemicals used were of highest purity available. Unless otherwise mentioned, all experiments were performed in 10 mM phosphate buffer pH 7.4.

Preparation of methionine-oxidized beta-lactoglobulin

1% w/v β-lg was oxidized with *t*-BHP (7.77 mM) by incubating the mixture for 5 days at room temperature. As *t*BHP control solutions were also incubated under identical conditions. The selected concentrations render to oxidize Met residues only while suppressing the oxidation of other oxidation-prone amino acids.[31] β-lg was precipitated by adjusting the pH to 2.6 followed by the addition of NaCl (30%, w/v). Protein was collected after centrifugation at 3300 × *g* for 15 min at 4 °C and resuspended and dialyzed against water for 3 days at 4 °C. Then, the protein samples were frozen at −10 °C and lyophilized using EYELA Freeze Dryer System (FDU-1200 JAPAN). Dry protein samples were stored at 4 °C for further use. 12% SDS-PAGE was performed with β-lg and ox-β-lg (ox-β-lg) solutions under non-reducing condition to compare electrophoretic mobility.

Preparation of β-lg and ox-β-lg samples for thermal incubation

163 μM of β-lg and ox-β-lg were incubated at 37 °C, 65 °C and 80 °C for 4 h to compare the aggregation behaviours of the two aforementioned samples. It is believed that molten-globule state was achieved by β-lg when incubated at 65 °C and β-lg undergoes aggregation readily upon thermal exposure at 80 °C when 163 μM of β-lg was used.[32,33]

Thermal aggregation study

Thioflavin T (Th T) assay. Thioflavin T (Th T) is a dye which shows enhanced fluorescence at around 480 nm when bound to amyloid fibrils.[34] Thus to investigate and compare the aggregates formed by incubated β-lg and ox-β-lg at 37 °C, 65 °C and 80 °C for 4 h, the following Th T assay was employed. Briefly 250 μL of β-lg and ox-β-lg samples (native and incubated) having concentrations 54.3 μM were mixed thoroughly with 1.75 mL of 50 μM Th T solution (stock 1 mM Th T in 20 mM sodium phosphate buffer, pH 7.5) and incubated for 30 min. The solution was excited at 440 nm and the emissions were measured over the range 455–600 nm. All the samples were blank corrected. Three replicates were performed and the data were averaged.

ANS fluorescence study

Exposure of hydrophobic patches in protein during the aggregation process was monitored using polarity sensitive fluorescent probe ANS.[35] A stock solution of ANS was added to each aliquot of incubated (37 °C, 65 °C and 80 °C) β-lg and ox-β-lg solutions so that the final ANS concentration in each aliquot was 30 mM. Typically, ANS concentration was 50 molar excess of protein concentration. The ANS-fluorescence intensities were measured with excitation at 370 nm and the emission recorded from 400 nm to 650 nm. Each spectrum was blank corrected. Data points were the average of triplicate measurements.

Rayleigh light scattering

The effect of methionine oxidation on the aggregation of β-lg was monitored by Rayleigh Light Scattering (RLS) measurement by observing emission at 350 nm after exciting the all solutions at 350 nm. The fluorescence spectra were taken after incubation of β-lg and ox-β-lg at 37 °C, 65 °C and 80 °C for 4 h. This

experiment was performed using a protein concentration of 13.6 μM. The excitation and emission slits were set at 3 nm.

Analysis of secondary structures by CD spectroscopy

To assess the secondary structural changes that methionine oxidation might induced on β-lg, circular dichroism measurements (CD) were carried out on a Jasco Spectropolarimeter (J-815) at 25 °C in the far-UV (200–260 nm) using quartz cuvette of 2 mm path-length. Thermally incubated β-lg solutions and ox-β-lg solutions having concentrations 13.6 μM were used for far-UV CD measurements. The final spectra were obtained after the subtraction of corresponding solvent spectrum. The percent of secondary structures present in β-lg and ox-β-lg under different conditions are determined by a curve-fitting program CDNN 2.1.

Congo red assay

The formation of aggregates by incubated β-lg and ox-β-lg solutions at 37 °C, 65 °C and 80 °C for 4 h can be investigated by measuring the shift in absorbance of Congo red in the region 400–700 nm. Congo red stock solution (10 mM) was prepared by dissolving the dye in 10 mM sodium phosphate buffer (pH 7.0) containing 150 mM NaCl under continuous stirring and filtered with a 0.2 mm Millipore syringe filter. A fresh working solution was prepared by diluting the stock solution 100 times. For this study, 250 μL (27.2 μM) aliquots of the protein solutions were mixed with 250 μL of a solution containing 40 μM Congo red solutions and total volume (2 mL) was adjusted with 10 mM sodium phosphate buffer, pH 7.4.

Dynamic light scattering (DLS) measurements

Dynamic light scattering (DLS) is a reliable technique to monitor aggregation in protein solutions and as well as size of particles. DLS measurements were performed with thermally incubated β-lg and ox-β-lg samples (37 °C, 65 °C and 80 °C) by employing Zetasizer Nanos (Malvern Instrument, UK) equipped with 633 nm laser and using 2 mL rectangular cuvette (path length 10 mm). Measurements were carried out at 20 °C by taking 250 μL of β-lg and ox-β-lg samples in 1.75 mL 10 mM sodium phosphate buffer (pH 7.4). The time-dependent auto correlation function was acquired with twelve acquisitions for each run.

Monitoring of secondary structures of β-lg during thermal incubation by FTIR spectroscopy

For FTIR measurements, β-lg and ox-β-lg solutions (native and thermally incubated) having concentrations 1087 μM were taken in a microcon filter device and diluted with 200 μL of D_2O. It was then quickly centrifuged at 4000 × *g* for 10 min until the volume reached ~50 μL. After that 200 μL of D_2O was added again and centrifuged for another 8–10 min. This process of D_2O exchange was repeated 3–4 times.[36] Finally, the D_2O exchanged β-lg samples were placed between two CaF_2 windows separated by a 50 μm thick Teflon spacer. FTIR scans were collected in the range of 1400–1800 cm^{-1} at a resolution of 2 cm^{-1} in N_2 environment using a Spectrum 100 FTIR spectrometer (PerkinElmer). Spectrum of D_2O at pD 7.5 was collected and subtracted from sample spectrum.

Morphological studies with FESEM and TEM

Field emission scanning electron microscope (FESEM) study. The morphology of the aggregates of β-lg and ox-β-lg (incubated at 80 °C for 4 h) were investigated using FE-SEM (Hitachi S-4800, JAPAN) operating with a voltage of 20 kV. For this study the concentrations of proteins were maintained at 40 μM. One drop of the sample solution was taken on a glass slide. It was dried by slow evaporation in open air and then under vacuum and gold coated for imaging.

Transmission electron microscopy (TEM). The morphology and size of the aggregates of β-lg and ox-β-lg obtained after incubation at 80 °C for 4 h were investigated by high resolution transmission electron microscopy (Jeol-HRTEM-2011, Tokyo, Japan) with an accelerating voltage of 80–85 kV in different magnifications. The sample solutions were diluted 50 times in 10 mM phosphate buffer of pH 7.4. A droplet of the diluted sample was put on a carbon coated copper grid of mesh size 300C (Pro Sci Tech). After 20 s the droplet was removed with a filter paper followed by a droplet of 2% uranyl acetate (Sigma, Steinheim, Germany) solution put on the grid and finally removed after 15 s and left for air dry and used for imaging purpose.

Results and discussions

We have performed all studies by selecting a model carrier protein β-lg *in vitro*. A study by Behl *et al.* suggested that *t*BHP is believed to be metabolized to produce *tert*-butoxyl free radicals and is a contact skin-irritant by dermal exposure and esophagus by oral administration in Fischer F344/N rats and B6C3F1 mice.[37] Although a few reports have been found on systemic toxicity of *t*BHP for *in vitro* studies from mammalian cell lines and *in vivo* studies, a proper toxicological characterisation of *t*BHP is still unknown. Also, we did not use any cell cultures to check toxicological profile of *t*BHP in our work.

t-Butyl hydroperoxide (*t*-BHP) is found to produce adverse effects in different systems. A recent study by Yeh *et al.*, reported a dose dependant effect of *t*BHP in rat aortic endothelial cells and thoracic aorta. It has been observed that in presence of *t*BHP decreased cell viability, affects cell toxicity, and prompted apoptosis and necrosis.[38] Thus, *t*-BHP is believed to be a major factor for impairing aortic endothelial cell survival and worsening vascular dysfunction. It has also been found that reactive oxygen species produced by *t*BHP reduce sperm parameters and testis cell viability of adult male mice and thus responsible for male infertility.[39]

Characterization of oxidized β-lactoglobulin (ox-β-lg)

SDS-PAGE analysis. SDS-PAGE was employed to ascertain the mass change upon oxidationunder non-reducing condition. Fig. S1 (ESI S1†), Panel S1 showed native β-lg bands (lane 5, 6 and 7) with corresponding molecular weight of ~18.3 kDa. The

mass of native β-lg was later confirmed by mass spectrometric data analysis. In ox-β-lg sample, a broadening of the band (lane 2, 3 and 4) at this molecular weight is observed highlighting the presence of slightly higher molecular weight components in the sample. In particular, it is possible to distinguish roughly two set of lanes. The difference in migration behaviour clearly indicates that some modification has been imparted in ox-β-lg due to *t*BHP treatment.

Mass spectrometric (MS) characterization

The ox-β-lg sample was analysed by MALDI-MS to confirm the oxidation of β-lg methionine residues. A portion of the raw mass spectra of oxidized β-lg are presented in Fig. 1A and S2A.† The molecular weight of native β-lg is reported as 18 300 Da.[40] Met oxidation is confirmed by an addition of mass ~48.514 Da (Fig. S2A†). Interestingly, Met7 is only surface-exposed and therefore susceptible to oxidation upon *t*-BHP treatment. On the contrary, partial oxidation may occur for other partially buried methionine residues in the protein core. The increment of molecular mass 48.514 Da corresponds to the formation of three possible methionine sulfoxides in β-lg.[28]

NMR spectroscopic evidence for oxidation

The 1D ^{1}H NMR spectra of native and oxidized β-lg are almost similar. A typical resonance shift at 2.9 ppm in the ^{1}H NMR spectra of oxidized β-lg [Fig. S3†] corresponds to the ε-methyl protons of oxidized methionine. The downfield shift from 2.75 ppm (native β-lg) to 2.9 ppm is observed due to the introduction of the electronegative oxygen to the sulphur atom (Fig. S3†). The ε-methyl proton of an oxidized Met residue resonating at higher δ-value is an indication of Met oxidation.

Intrinsic fluorescence study

Spectroscopic properties of both β-lg and oxidized β-lg (ox-β-lg) were compared to understand the impact of Met oxidation induced on the protein structure and conformation. Intrinsic fluorescence spectra of β-lg (profile a) and ox-β-lg (profile b) are shown in [Fig. 1, Panel A]. The two tryptophan residues of β-lg, Trp_{19} and Trp_{61}, provided information to assess the protein's conformational state. The intrinsic fluorescence of Trp_{61} is significantly quenched by the close proximity of the neighbouring disulphide bond, Cys_{160-66}.[41] As a consequence, Trp_{19} is solely responsible to provide a probe for tryptophan fluorescence of β-lg with a small contribution of tyrosine.

In particular, fluorescence intensity of ox-β-lg is increased with slight red-shift (~3 nm ± 0.02). It may be due to the incorporation of oxygen atom which provides more polar environment, ultimately causing the tertiary structure modification of protein. As a consequence, the data in Fig. 1, Panel A reveals that oxidation of β-lg led to an increase in fluorescence through exposure of protein chain into a more flexible structure [Fig. 1, Panel A, profile b] in such a way that Trp_{19} achieved more hydrophobic environment.[42]

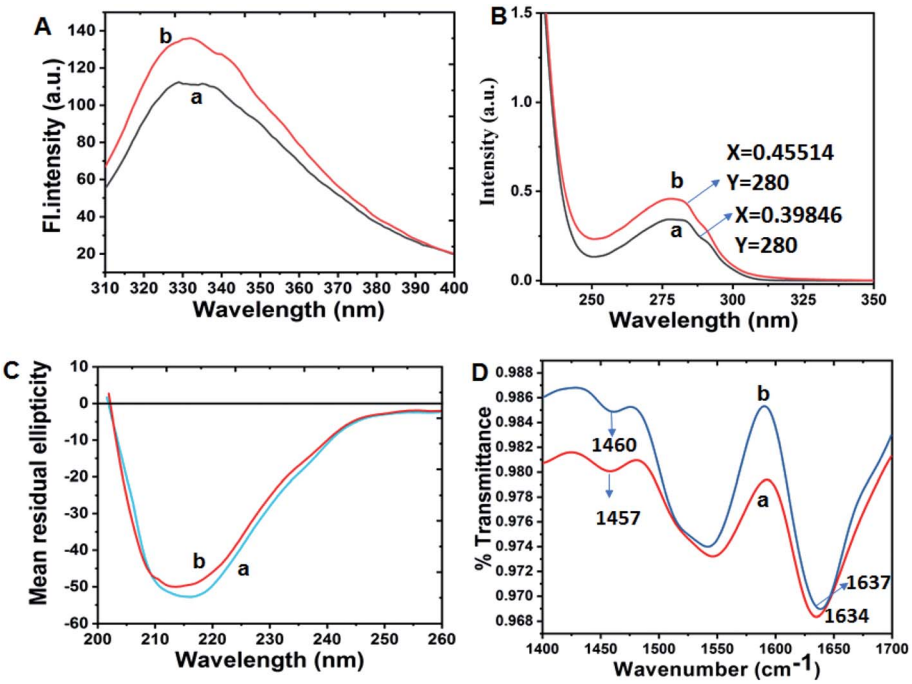

Fig. 1 Panel A: intrinsic fluorescence spectra of native β-lg (profile a) and ox-β-lg (profile b) in 10 mM phosphate buffer at pH 7.4 at room temperature. The excitation wavelength was 295 nm and emission spectra were recorded between 310 nm and 400 nm. The excitation and emission slits were set at 3 nm and 5 nm respectively. Panel B: ultraviolet (UV) absorption spectra of β-lg (profile a) and ox-β-lg (profile b) in 10 mM phosphate buffer at pH 7.4 at room temperature. Panel C: far-UV CD spectra of native β-lg (profile a) and ox-β-lg (profile b) in 10 mM phosphate buffer at pH 7.4 at room temperature. Both the sample concentrations were kept at 13.6 μM. Panel D represents FTIR spectra of β-lg (profile a) and ox-β-lg (profile b) in D_2O in the amide region (1400–1700 cm^{-1}). Both the sample concentrations were kept at 1087 μM.

UV-spectral characterization

In order to compare structural changes around the chromophores after mild oxidation, both native β-lg and ox-β-lg samples were subjected to UV-spectral studies at 280 nm. Fig. 1, Panel B showed a little change in the absorption spectra for both samples. Therefore, microenvironment of Trp_{19} residue is believed to change in presence of *t*BHP.

Effect of methionine oxidation on conformational changes of β-lg and oxidized β-lg (ox-β-lg)

In order to determine secondary structural alteration of β-lg upon *t*BHP treatment, far- and near-UV CD spectra of native β-lg was compared with that of ox-β-lg. The native β-lg [Fig. 1, Panel C, profile a] exhibits negative minima at around 216 nm and 207 nm which are characteristics for the β-sheet structure of the β-lg along with some α-helical conformation.[43] The reduction of β-sheet content approximately from 39% to 35% in the far-UV region [Fig. 1, Panel C, profile b] indicates that oxidation of β-lg led to the formation of a molecule with less organized secondary structure compared to native β-lg.

On another note, the change of near-UV CD spectrum of ox-β-lg (Fig. S4†) indicating that the chiral microenvironments of aromatic residues are also significantly altered due to oxidation. Therefore, it appears that oxidation of accessible methionine residues disrupts the global structure of β-lg.

Additionally, it may be possible that the native tertiary structure is destabilized by the introduction of more hydrophilic residues at the non-polar face of protein, which could lead alteration of solution conformation of β-lg. As Met7 is exposed and Met24, Met107 are partially buried, therefore promoting local increase of hydrophilicity upon *t*BHP treatment, may subsequently disrupted hydrophobic interactions, and thus causing unfolding of the protein.

Characterization by FTIR spectra

It is believed that *t*BHP-induced oxidation takes place for solvent-exposed and partially buried methionine residues[10] and the peak at 1044 cm^{-1} is characteristic stretching vibration of S=O in methionine sulfoxide.[29,44] Furthermore, it has been demonstrated that for rt-PA and IFN-γ, only solvent exposed amino acid are were oxidized in the presence of *t*-BHP.[29] In Fig. 1, Panel D, the FTIR spectra of β-lg (profile a) and ox-β-lg (profile b) are reported. The peak assigned at ~1634 cm^{-1} in amide-I region corresponds to intramolecular β-sheet structures of β-lg and at ~1450 cm^{-1} due to amide-II band.[45] As amide-I band gives information about secondary structural changes of protein, therefore, significant differences in secondary structures can be detected in the amide I region (1600–1700 cm^{-1}). Fig. 1, Panel D indicates that the peak at ~1634 cm^{-1} shifted to ~1637 cm^{-1} upon oxidation. A clear difference was observed in amide-II region (1450–1550 cm^{-1}). The amide II/II′ band is sensitive to the H/D exchange of amide groups and may therefore infer structural compactness and flexibility of protein.[46,47] In particular, H/D exchange in the amide-II region provides important information on the amount of hydrogen atoms situated in the protein core. The ratio between the two peaks is more pronounced for ox-β-lg. This result infers that *t*BHP-induced oxidation directs a probability of solvent accessibility to the internal protein core, possibly leading to a more flexible structure.

ANS titration study

A thorough study is carried out with 8-anilino-naphthalene sulfonic acid (ANS), a molecule possesses both hydrophilic and hydrophobic characters and whose fluorescence serves as a sensitive tool to understand the nature of β-lg binding regions.[48] In particular, the bindings of β-lg and ox-β-lg to ANS were analysed by titration and the results are plotted in the Fig. 2, Panel A. Two potential binding sites in β-lg have been postulated for hydrophobic ligand binding: one of these sites, "site 1," is an "internal" site localized in the beta barrel of the protein and it is the putative site for ligands such as retinol, dodecanoic acid, and palmitate. The other site, "site 2," is a "surface" site located near the interface between the beta barrel and the alpha helix, away from the dimer interface.[45] However, ANS seems to reasonably fit in the beta-barrel, in agreement with the observed binding which shows intermediate strength.[49] Fig. 2, Panel A shows the emission spectrum of ANS as a function of increasing [ANS]/[protein] molar ratio for both β-lg (profile a) and ox-β-lg (profile b) samples. Similar trend of ANS intensity was observed for both the samples, it increased at first and then a plateau was observed. The presences of the two sites of β-lg attribute the biphasic behaviour in the titration curves. Specifically, for β-lg up to a molar ratio [ANS]/[protein] of about 1.0, ANS interacts predominantly with the higher affinity binding site located in the beta-barrel, while, at higher ANS concentration, the dye occupies both binding sites.[50] Similar trend is observed for ox-β-lg up to [ANS]/[protein] is 0.7. Significant differences are observed for higher molar ratios, in which the binding site located near the interface between the beta barrel and the alpha helix away from the dimer interface. These data suggest that oxidation induced by *t*BHP increase the accessibility of hydrophobic sites of β-lg. Since Met_7 is one of the most oxidation-prone residues, therefore, methionine residue is likely oxidised. Docking studies based of MIFs analysis shows that ANS molecule selectively attached at the cavity with anilino group positioning within the internal cavity and negatively charged sulphonate group remains closed contact with surrounding Lys_{60} and Lys_{69} residues.[51] It is important to note that, Met_{24} and Met_{107} residues are also susceptible to partial oxidation located in close proximity of ANS binding site. As a consequence, oxidation of these methionine residues may increase hydrophobicity of the surface exposed side chain, leading to ANS binding affinity in this region due to structural alteration.

Fibril-forming propensity of native β-lg and oxidized β-lg (ox-β-lg)

Identification and quantification of amyloid fibrils by Th T assay. Thioflavin T (Th T), a benzothiazole dye, selectively interacts with amyloid fibrils leading to an increase in the

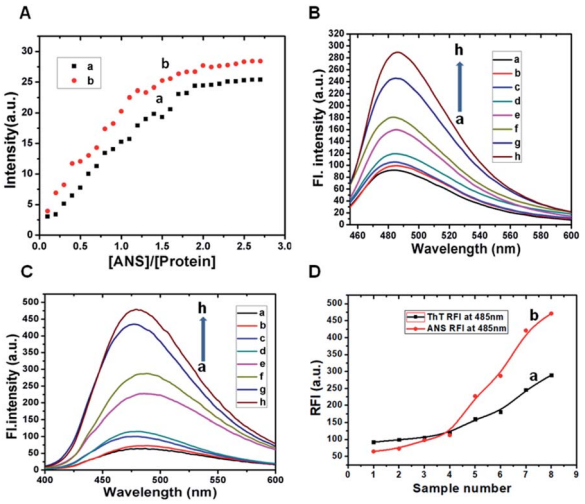

Fig. 2 Panel A: ANS titration curves: integrated intensity of ANS emission as a function of molar ratio [ANS]/[protein] for β-lg (a) and ox-β-lg (b) in the range [ANS]/[protein] = 0.1–2.8. ANS fluorescence was measured at room temperature using an excitation wavelength λ_{ex} = 380 nm with β-lg and ox-β-lg samples in 10 mM phosphate buffer at pH ~ 7.4. Panel B: Th T assay of native β-lg (profile a), ox-β-lg (profile c), β-lg and ox-β-lg incubated for 4 h at 37 °C (profile b and profile d), 65 °C (profile e and profile f) and 80 °C (profile g and profile h) respectively. Fluorescence emissions were monitored in the wavelength range 455–600 nm after excitation at 440 nm. Panel C: ANS fluorescence of native β-lg (profile a), ox-β-lg (profile c), β-lg and ox-β-lg incubated for 4 h at 37 °C (profile b and profile d), 65 °C (profile e and profile f) and 80 °C (profile g and profile h) respectively. Excitation was done at 370 nm and emissions were measured in the wavelength range 400–600 nm. Proteins concentrations during ANS fluorescence and Th T assay were 13.6 μM. Panel D represents relative fluorescence intensities of Th T assay (profile a) and ANS fluorescence (profile b) at 485 nm. The points in profile a and profile b represents maximum intensities at 485 nm from curve a → h of Panel A and Panel B respectively.

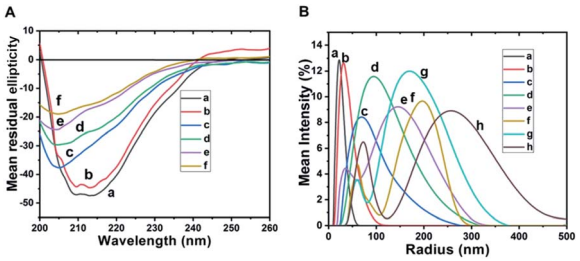

Fig. 3 Panel A represents far UV-CD spectra of β-lg and ox-β-lg incubated for 4 h at 37 °C (curve a and curve b), 65 °C (curve c and curve d), and 80 °C (curve e and curve f) respectively in 10 mM phosphate buffer at pH 7.4. Concentrations of β-lg and ox-β-lg samples in far UV-CD measurements were 13.6 μM. Panel B represents number particle size distribution spectra in DLS studies of native β-lg (line a) and ox-β-lg (line b) and β-lg and ox-β-lg incubated for 4 h at 37 °C (line c and line d), 65 °C (line e and line f) and 80 °C (line g and line h) respectively. Each spectrum is an average of 48 scans. Protein concentrations for DLS studies were 54.3 μM.

fluorescence intensity at around 480 nm.[52] Fig. 3, Panel B shows a comparative study of the aggregation patterns of non-oxidized and oxidized β-lg as monitored by Th T fluorescence. However, in our experiments, β-lg and ox-β-lg samples were incubated in three different temperatures such as 37 °C, 65 °C and 80 °C for 4 h to compare thermal stability and their propensities for aggregate formation. It can be demonstrated that *in vitro*, the process of fibril formation upon oxidation was faster than in the native state. Therefore, the increased intensity of Th T fluorescence for oxidized β-lg at different temperatures may correlate the formation of more aggregated species. The observed increase in Th T intensity for ox-β-lg with the increasing temperature is consistent with the nucleated elongation mechanism for most amyloid fibril formation. The reduced protein stability and structural compactness generated due to the oxidation may modify the balance between stabilizing interactions including hydrogen bonding, hydrophobic interactions, electrostatic forces and ultimately increases aggregation propensity.[53,54] We assume that *t*BHP-induced perturbations of the tertiary structure may cause acceleration of protein aggregation by increasing the population of partially unfolded, aggregation-prone residues. However, our result differs with the report of Sancataldo *et al.* (2014), where it has been found that oxidized HSA has higher thermal resistance compared to the native protein.[21]

Detection of exposed hydrophobic clusters by ANS binding

To monitor hydrophobic interactions involved in the aggregation processes, ANS fluorescence experiment was performed. The intensity of ox-β-lg (Fig. 2, Panel C, profile d) was higher than native β-lg (Fig. 2, Panel C, profile b) when the samples were incubated at 37 °C. The intensity measured at 65 °C at the beginning of aggregation process is significantly higher for ox-β-lg sample (Fig. 2, Panel C, profile f) compared to β-lg (Fig. 2, Panel B, profile e). The results suggest that oxidation induces conformational changes in the proximity of ANS binding sites. The enhancement of ANS fluorescence intensity indicates an increased interaction of the dye with suitable hydrophobic binding sites and this increase in intensity is usually accompanied by the blue shift of the fluorescence emission band. The maximum fluorescence intensity was 435 a.u. at 480 nm for incubated β-lg at 80 °C (Fig. 2, Panel C, profile g) which increased to 480 a.u. for ox-β-lg at identical condition (Fig. 2, Panel C, profile h). It is of interest to note that, the oxidation of methionine led to an increase in fluorescence of the hydrophobic probe ANS presumably through localized unfolding of the protein, leading to greater exposed, clustered regions of hydrophobicity at the protein surface. The enhanced surface hydrophobicity promotes aggregation behavior of oxidized β-lg.

Identification of aggregation by Rayleigh Light Scattering (RLS) measurements

Rayleigh Light Scattering (RLS) measurement is a selective method to investigate protein aggregation. RLS data were collected after incubation of β-lg and ox-β-lg solutions at 37 °C, 65 °C and 80 °C for 4 h. Our results as shown in the Fig. S5† indicate that the aggregation process is accelerated by oxidation. In addition, it is worth to point out that maximum

scattering intensity is observed for incubated ox-β-lg at 80 °C suggesting maximum aggregate formation at this higher temperature. It can be demonstrated that oxidation might also loses the structural integrity of the protein and thus alters the amyloid self-assembly and aggregation profile.

CD spectroscopic analysis to assess secondary structural changes

In order to assess secondary structural changes in the aggregation process, we followed the changes of far UV-CD spectra with temperature. Fig. 4, Panel A shows the far UV-CD spectra of β-lg and ox-β-lg samples measured at 37 °C, 65 °C and 80 °C after incubation for 4 h. Curve a in Fig. 4, Panel A represents that the CD spectra of incubated β-lg at 37 °C is very similar with native β-lg (as shown earlier). On the other hand, the CD spectra for incubated ox-β-lg at 37 °C (Fig. 3, Panel A, curve b) display quite different nature compared to ox-β-lg (as shown earlier). It is manifested by the decreased negative ellipticity in the vicinity of 210 nm. Incubation at 65 °C, the random coil and β-sheeted structures are predominating for the ox-β-lg (Fig. 3, Panel A, curve d) compared to incubated β-lg at the same temperature (Fig. 3, Panel A, curve c).

The aggregates of incubated β-lg at 80 °C (Fig. 3, Panel A, curve e) are found to have even more beta and random coil with lesser α-helical structure than the native. In particular, for incubated ox-β-lg at 80 °C that there is a gradual loss in the negative ellipticity of the CD signal (Fig. 3, Panel A, curve f). Therefore, systematic loss in CD signal is an indicative of self-assembly formation.[52] It is important to note that; ox-β-lg is conformationally less stable than the native protein, thus unfolded readily during thermal stress. Based on Lumry–Eyring mechanism, structurally flexible and conformationally fewer stable proteins are believed susceptible to aggregation.[55] Also, it has been reported by Danny *et al.* that methionine oxidation by *t*BHP causes exposure of Albinterferon (Al fa-2b) hydrophobic interior.[56] It should be pointed out that, under the same experimental conditions, aggregation of β-lg and ox-β-lg occurs *via* different pathways involving different conformational changes.

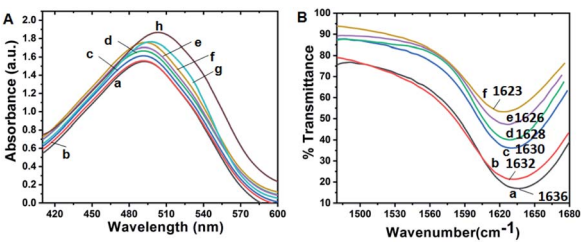

Fig. 4 Panel A represents Congo red absorption spectra of native β-lg (line a) and ox-β-lg (line c) and β-lg and ox-β-lg incubated for 4 h at 37 °C (line b and line d), 65 °C (line e and line f) and 80 °C (line g and line h) respectively in 10 mM sodium phosphate buffer pH-7.4. The absorption spectra were recorded from 400 to 600 nm. The protein concentration for Congo red absorption spectra was 27.2 μM. Panel B represents Fourier transform infrared (FTIR) spectra of incubated β-lg and ox-β-lg for 4 h at 37 °C (line a and line b), 65 °C (line c and line d) and 80 °C (curve e and curve f) in 10 mM sodium phosphate buffer pH-7.4. Protein concentrations were 1087 μM. Each spectrum is an average of 32 scans in D_2O solvent at 25 °C.

DLS study

Dynamic light scattering (DLS) was unambiguously used to identify heat-induced aggregation process of β-lg. We examined the size distribution profile of native β-lg and ox-β-lg at 37 °C, 65 °C and 80 °C after incubation for 4 h. The hydrodynamic radius of native β-lg was ranging from 12 nm to 50 nm (Fig. 3, Panel B, line a) while the hydrodynamic radius of ox-β-lg was ranging from 15 nm to 100 nm (Fig. 4, Panel B, line b). On the basis of the present data, it is easy to discriminate aggregation patterns of β-lg and ox-β-lg upon thermal incubation. Notably, on thermal incubation at 37 °C, the monomers of β-lg are converted into dimeric state and their size ranging from 25 nm to 250 nm (Fig. 3, Panel B, line c). On the other hand, the monomers of ox-β-lg when converted into dimeric or trimeric state, their size ranging in between 25 nm to 300 nm (Fig. 3, Panel B, line d). However, upon thermal incubation at 65 °C, the enhancement of hydrodynamic radius of ox-β-lg (Fig. 3, Panel B, line f) with respect to β-lg (Fig. 3, Panel B, line e), might be indicative of acceleration of the aggregation processes. This result could mainly be attributed to oligomeric states or protofibrillar states of protein. Importantly, the formation of larger aggregates at 80 °C was also more prominent in the oxidized samples (Fig. 3, Panel B, line h) compared with the non-oxidized protein. Significantly, greater hydrodynamic radius was observed for oxidized β-lg compared to β-lg at 80 °C (Fig. 3, Panel B, line g) (size ranging from 30 nm to 375 nm), which correlated with formation of larger aggregates for oxidized β-lg (size ranging from 30 nm to 500 nm) (Fig. 3, Panel B, line h). It has also been demonstrated that oxidation of HSA results greater exposure of hydrophobic regions and causing aggregation.[57,58]

Congo red assay

Congo red (CR) spectral shift assay is extensively employed to measure fibril content of protein. On the chemical point of view, two binding sites of CR have been detected in amyloid such as parallel to the β-sheet and antiparallel to the β-sheet.[59] Specific binding of the dye to the cross β-sheet region led to an increased absorption along with bathochromic shift (red shift) in absorption spectrum. The CR assay was performed by incubating β-lg and ox-β-lg at 37 °C, 65 °C and 80 °C for 4 h. In general, native β-lg exhibited absorption maxima at 493 nm (Fig. 4, Panel A, line a). No significant change of absorption spectrum of β-lg is observed upon incubation at 37 °C (Fig. 4, Panel A, line b). On the contrary, the ox-β-lg (Fig. 5, Panel A, line c) shows increase in absorption upon incubation at 37 °C (Fig. 4, Panel A, line d). Interestingly, the absorption spectra at 65 °C of the bound CR can provide information about the modulation of aggregation process by ox-β-lg (Fig. 4, Panel A, line f).

Upon interacting with cross β-sheet-rich fibrillar aggregates, a red shift was observed for ox-β-lg (λ_{max} shifts from 493 nm unbound to 504 nm bound) (Fig. 4, Panel A, line h) with respect to β-lg during incubation at 80 °C (λ_{max} shifts from 493 nm

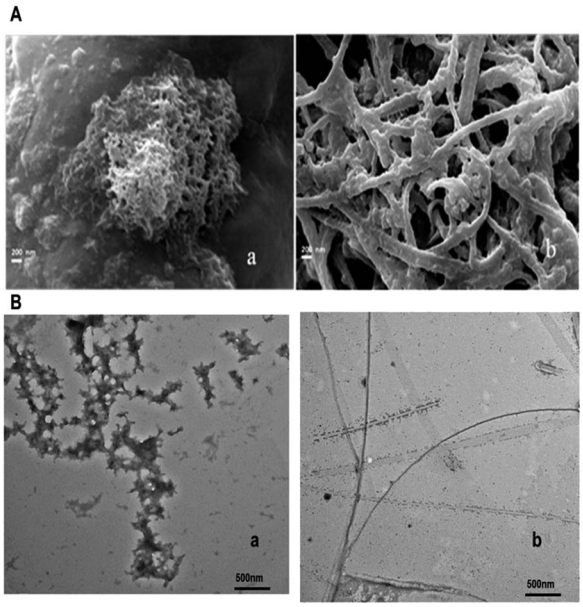

Fig. 5 Panel A: FE-SEM images showing the formation of distinct self-assembled structure of β-lg (image a) and ox-β-lg (image b) upon incubation at 80 °C for 4 h in 10 mM phosphate buffer at pH 7.4. Panel B: TEM images of β-lg (image a) and ox-β-lg (image b) aggregates upon incubation at 80 °C for 4 h in 10 mM phosphate buffer at pH 7.4.

unbound to 500 nm bound) (Fig. 4, Panel A, line g). It is of interest to note that, β-lg and ox-β-lg modulate the fibril formation processes in a temperature-dependent fashion.

FTIR study to monitor secondary structural changes

Fourier transform infrared (FTIR) spectroscopic technique is one of the most convenient tools to determine the secondary structure and conformational changes of protein due to aggregation. During incubation at 37 °C for 4 h, the peak of β-lg shifts from 1634 cm^{-1} to 1636 cm^{-1} due to small changes in secondary structures (Fig. 4, Panel B, line a). On the other hand, incubation at 37 °C, shifts the peak of ox-β-lg from 1637 cm^{-1} to 1632 cm^{-1} (Fig. 4, Panel B, line b) is observed. For incubated β-lg at 65 °C, the amide-I peak at 1630 cm^{-1} corresponds to intermolecular β-sheet structures (Fig. 4, Panel B, line c). The peak at 1628 cm^{-1} for incubated ox-β-lg indicates β-sheeted structure (Fig. 4, Panel B, line d). Upon incubation at 80 °C, the amide-I peak of β-lg again shifts to a lower wave number 1626 cm^{-1} (Fig. 4, Panel B, line e). On the contrary, when ox-β-lg was incubated at 80 °C, the amide-I band shifts at 1623 cm^{-1} (Fig. 4, Panel B, line f). Such gradual lowering of stretching frequency indicates the gradual formation of non-native β-sheet structure (intermolecular rather than intramolecular) during aggregation, which is the hallmark of amyloid-like fibrils formation.[60] Thus, oxidation resulted in an increase in fibril forming propensity.

Morphological studies with SEM and TEM

The morphology of the aggregates of β-lg and ox β-lg generated on incubation at 80 °C for 4 h are shown in the Fig. 5, Panel A (image a and b). The SEM image of β-lg show distinct self-assembled structure with fibrillar aggregates on incubation at 80 °C for 4 h (Fig. 5, image a). In contrast, elongated fibrillar networks are formed when ox-β-lg incubated at 80 °C for 4 h (Fig. 5, image b).

To better examine the effect of oxidation in modulating the fibrillar assembly of β-lg, ultrastructural morphologies are obtained after incubation of β-lg and ox-β-lg at 80 °C for 4 h. TEM images of β-lg and ox-β-lg aggregates are shown in Fig. 5, Panel B (image a and b) in order to assess the overall differences qualitatively in formation of mature aggregates. It has been observed that β-lg formed worm-like (approximate diameter 40–55 nm) less fibrillar aggregates whereas a different rod-shaped aggregate (apparent diameter 20–35 nm) with a high degree of fibril structure was formed for ox-β-lg upon incubation at 80 °C for 4 h (Fig. 5, Panel B, image b). The formation of the fibrillar structure suggests that the protein acquires a highly flexible structure upon oxidation.

The different conformational changes possibly modulate the secondary structures leading to cross β-structure formation and ultimate ultrastructural morphologies. However, it has been proposed that suppression of fibril formation of apolipoprotein C-II due to oxidation of Met is subjected to hydrophobic interactions of Met residue within the fibril core structure which are drastically altered by more hydrophilic Met sulfoxide side chain.[19] For instances, oxidation prone Met35 and Met60 lie in the core fibril region of Aβ16 and apolipoprotein C-II,[19] respectively. Mass spectroscopic analysis of major peptide fragments of β-lg revealed that fractions 135–158 are mainly responsible for formation of aggregates[61] which may exclude the role of oxidation of Met7, Met24 and Met107 in suppression of fibrillation. It is worth mentioning that, opposite trend is also observed in case of α-synuclein, where Met1, Met5, Met116, and Met127 positioned outside of its fibril forming core and fibrillation is inhibited due to oxidation.[20] In our experimental conditions, Met oxidation facilitates the formation of partially unfolded structure with greater exposure of aggregation-prone residues possibly with indirect involvement of modified amino acids in hydrophobic packing in the fibril forming region with ability of unique hydrogen bonding formation and enhanced noncovalent interactions, as likewise behavior of amyloidogenic peptides.[62] Interestingly, heat induced aggregation of ox-β-lg results a probable change in orientation of Trp61 due to relaxation of quenching effect and initiates the self-assembled structures by close contact of free thiol group which are involved in forming region with ability of unique hydrogen bonding formation and enhanced noncovalent interactions, as likewise behavior of amyloidogenic peptides.[63] Interestingly, heat induced aggregation of ox-β-lg results a probable change in orientation of Trp61 due to relaxation of quenching effect and initiates the self-assembled structures by close contact of free thiol group which are involved in forming rapid intermolecular S–S bond compared to unmodified β-lg in a temperature dependent manner. Similar findings were also reported by Feng *et al.* (2014), where methionine oxidation reduces structural stability and subsequently enhances aggregation propensity of human prion protein.[64] Recently, several

reports on methionine oxidation have attracted great attention.[65,66]

Theoretical study

The molecular electrostatic potential map of *t*BHP molecules (Fig. S5†) was calculated from its optimized structure to understand its capability of interaction from electrostatic behavior. The studies show that, in *t*BHP, the oxygen atoms are buried inside the hydrophobic shell made with methyl groups (green region in Fig. S6†) and has a strong acidic proton (blue region in Fig. S6†) available for hydrogen bonding. Therefore, *t*BHP have capability of oxidation inside the hydrophobic region of the protein through binding.

Docking study is a tool, generally used to predict the position and binding interactions of molecule into proteins or DNAs.[67,68] Among the four methionine amino acids of β-lg, Met7 is located at the surface of the protein and easy to oxidize, Met24 and Met107 are located inside the hydrophobic calyx of β-lg and Met145 is also in the hydrophobic core (Fig. 6). Here, we utilized the docking study to predict the available methionine amino acids for oxidation through finding the binding site of the *t*BHP in β-lg. This study shows that *t*BHP can bind with the protein through hydrogen bonding as well as hydrophobic interactions with those regions having Met7, Met24, and Met107 residues (Fig. 6) with comparable binding energy −3.78 kcal mol^{-1}, −2.81 kcal mol^{-1} and −2.58 kcal mol^{-1}, respectively. The close contact of *t*BHP with Met residues indicates that these three Met residues are oxidized preferentially, as revealed from mass spectroscopic studies. The oxidation of thiomethyl groups results the formation of a polar group sulfoxide groups. Therefore, the oxidation enhances the overall polarity of the ox-β-lg molecule with respect to β-lg which is responsible for the conformational change of the ox-β-lg protein to minimize the additional dipole moment as reflected in the CD and FT-IR studies. This conformational change is believed to unfold the ox-β-lg in such a way that the Trp19 can access more hydrophobic environment which enhance its fluorescence intensity as determined in fluorescence studies.

Compatibility

The amino acid composition, genetic polymorphism, structure and biological function of whey proteins in human milk are quite different compare to milk of other species. Human milk whey protein consists of alpha-lactalbumin, secretory immunoglobulins, lactoferrin, lactoperoxidase, lysozyme, osteopontin and serum albumin. The most abundant whey protein is alpha-lactalbumin, which contains higher levels of tryptophan, lysine, and cysteine than other proteins in human milk. Human milk whey proteins involved in immune response, cell communication, metabolism/energy production and general transport. Bovine milk contains less α-lactalbumin, lactoferrin, and osteopontin compare to human milk. The beta-

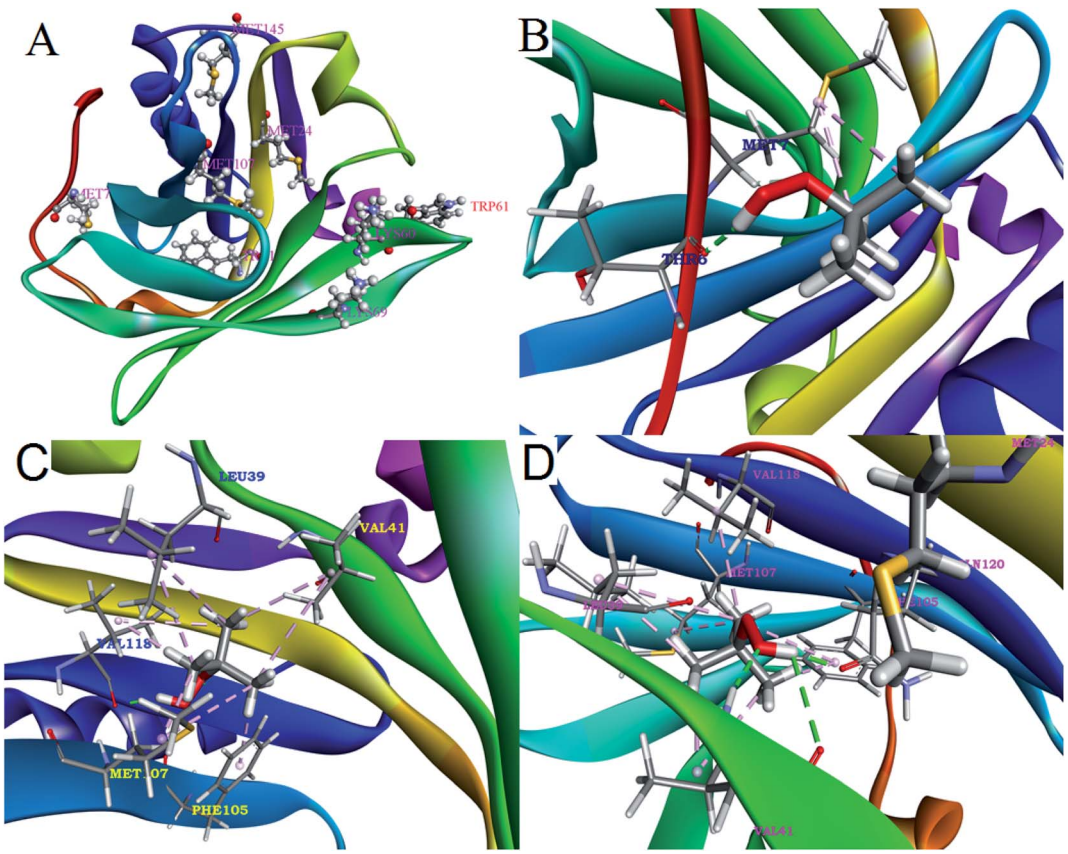

Fig. 6 Represents the structure of β-lg-*t*BHP with specific orientation of all methionine residues. Possible interactions contributing to the binding of β-lg with *t*BHP obtained by molecular docking (PDB ID of β-lg: 1BSY).

lactoglobulin is the major whey protein found in bovine milk. Bovine whey contains caseins (α_{s1}-, α_{s2}-, β- and κ-casein), but in human whey, casein present in lesser amount. The main biological properties including antimicrobial and antiviral actions, immune system stimulation, anticarcinogenic activity and other metabolic behaviours are associated with the bovine whey proteins. A study by Kuitunen *et al.*, showed that systmetic absorption of human alpha-lactalbumin and bovine beta-lactoglobulin does not happen in infants.[69]

Oxidative damage of whey proteins is related with the residues that are modified and are involved with the degree of protein unfolding. Interestingly, alpha-lactalbumin shows pronounced effect on oxidation than beta-lactoglobulin. It has been reported that with treatment of heat and hydrogen peroxide for alpha-lactalbumin and β-lgor mixture of both produce sulfenic acids, methionine sulfoxides and disulfide mono oxides of cysteine, methionine and disulfides. The oxidation of these residues cause protein unfolding and structural changes.[70] Although, a very few literatures of methionine oxidation of whey proteins have been found. It has been suggested that apolipoprotein A-I, apolipoprotein A-II, beta-casein, kappa-casein, serum albumin and a bunch of proteins were identified from human milk whey by proteomic analysis.[71] We have selected bovine β-lg because it is one of the mostly used accepted model carrier protein for hydrophobic ligands, having pH dependent opening, encapsulating property and a unique acidic pH resistivity. To the best of our knowledge, to date, the *in vitro* systematic study of methionine oxidation by *t*BHP and its impact on structural changes, fibril forming propensity of bovine β-lgis not yet performed properly. Our experimental results from bio-physical techniques are also supported by several another reports. It has been reported that oxidation of methionine residues of kappa-casein enhanced surface hydrophobicity and fibril forming propensity as determined by ANS and ThT fluorescence respectively. The fibrillar structural network upon oxidation was confirmed by TEM study. It has been suggested that the fibril-forming core of kappa-casein consists residues Tyr25–Lys86 which delineates oxidation of Met95 and Met106 may responsible for fibril formation as Met95 is located in the hydrophobic N-terminal domain and Met106 is located at the polar C-terminal domain.[23] In our experimental condition, subtle modifications increase surface hydrophobicity of beta-lactoglobulin and direct the formation of partially unfolded structure with greater exposure of aggregation-prone residues possibly with involvement of modified amino acids in hydrophobic packing in the fibril forming region. Our results were confirmed by employing several bio-physical techniques including ANS and ThT fluorescence, CD and TEM study. We demonstrate that *t*BHP can bind with β-lg through hydrogen bonding and hydrophobic interactions with regions having Met7, Met24, and Met107 residues which indicates preferential oxidation of these Met residues. A study by Wong *et al.*, reported that methionine oxidation of apolipoprotein A-I (apoA-I), a major protein component of HDL, caused misfolding and reduced thermal stability. Thioflavin T (Th T) and Congo red assay suggested fibrillar aggregates of apoA-I. Morphological studies of aggregates of oxidized apoA-I revealed ribbon-like structures.[22] In our experimental condition, rod-shaped morphology was found for oxidized b-lg. It has been demonstrated that the three methionine residues of apoA-I, Met86, Met112, and Met148 are situated on four-helix bundle domain and are involved in specific hydrophobic contacts. Another report by Sancataldo *et al.*, showed that oxidation of single Met residue of Human serum albumin (HSA) resulted in enhancement of thermal stability and decreases fibril forming propensity. For HSA, Met oxidation prevents amyloid fibril formation through the involvement of domain III.[21] Therefore, it is worth mentioning that environmental position of methionine residues may responsible for fibrillogenesis and in inhibition of fibril formation.

Conclusions

In summary, we report that *t*-BHP-induced selective Met oxidation affects structural orientation of β-lg, reducing its resistance against thermal stability and alters the internal polarity of the protein which introduce an internal strain.

It is worth noting that, whey protein modification due to methionine oxidation serve a key determinant in the dairy industry during milk processing, leading to reduce nutritional value and influence their technological properties.[72] Furthermore, Met modification has been presented a conundrum with a function of temperature. Therefore, our studies have great implications to understanding and explore the underlying mechanism of other whey protein modification encountering the oxidative stress (methionine oxidation). On another note, further investigations are needed for different milk proteins. Moreover, *in vivo* studies for potential stress-related proteins are required where Met oxidation is connected with other modifications as part of the cellular defence against oxidative stress and neurological disorders.

Author contributions

SM and UCH designed the work. SM and SP performed the work. SS, JC, HP and SP performed protein isolation and purification. FE-SEM, TEM images and NMR data are collected and analyzed by AP. NS performed theoretical studies. SM write the manuscript and SM and NS analyzed the data with assistance and feedback from all other.

Conflicts of interest

The authors declare no competing financial interest.

Acknowledgements

Financial support of University Grants Commission UGC-CAS-II and DST-PURSE-II (Govt. of India) Program of Department of Chemistry, Jadavpur University, Kolkata are greatly acknowledged. The authors wish to acknowledge Prof. S. C. Bhattacharya, Department of Chemistry, Jadavpur University for providing the DLS instrumental facility. SM was recipient of

UGC-SRF fellowship. AP acknowledges DST for funding through the INSPIRE program.

Notes and references

1 B. Halliwell, *J. Neurochem.*, 1992, **59**, 1609–1623.
2 D. A. Butterfield, J. Drake, C. Pocernich and A. Castegna, *Trends Mol. Med.*, 2001, **7**, 548–554.
3 R. Alvariño, E. Alonso, M. E. Abbasov, C. M. Chaheine, M. L. Conner, D. Romo, A. Alfonso and L. M. Botana, *ACS Chem. Neurosci.*, 2019, **109**, 4102–4111.
4 A. Dalrymple, E. J. Wild, R. Joubert, K. Sathasivam, M. Björkqvist, Å. Petersén, G. S. Jackson, J. D. Isaacs, M. Kristiansen, G. P. Bates, B. R. Leavitt, G. Keir, M. Ward and S. J. Tabrizi, *Proteome Res.*, 2007, **67**, 2833–2840.
5 J. D. Sipe, *Annu. Rev. Biochem.*, 1992, **61**, 947–975.
6 D. J. Selkoe, *Nature*, 2003, **426**, 900–904.
7 J. E. Duda, B. I. Giasson, Q. Chen, T. L. Gur, H. I. Hurtig, M. B. Stern, S. M. Gollomp, H. Ischiropoulos, V. M. Lee and J. Q. Trojanowski, *Am. J. Pathol.*, 2000, **157**, 1439–1445.
8 T. Lynch, R. A. Cherny and A. I. Bush, *Exp. Gerontol.*, 2000, **35**, 445–451.
9 W. R. Markesbery, *Free Radical Biol. Med.*, 1997, **23**, 134–147.
10 H. Ostdal, M. J. Bjerrum, J. A. Pedersen and H. J. Andersen, *J. Agric. Food Chem.*, 2000, **48**, 3939–3944.
11 W. Vogt, *Free Radical Biol. Med.*, 1995, **18**, 93–105.
12 Y. R. Hsu, L. O. Narhi, C. Spahr, K. E. Langley and H. S. Lu, *Protein Sci.*, 1996, **5**, 1165–1173.
13 J. L. Liu, K. V. Lu, T. Eris, V. Katta, K. R. Westcott, O. NarhiL and H. S. Lu, *Pharm. Res.*, 1998, **15**, 632–640.
14 D. Liu, D. Ren, H. Huang, J. Dankberg, R. Rosenfeld, M. J. Cocco, L. Li, D. N. Brems and R. L. Remmele Jr, *Biochem*, 2008, **47**, 5088–5100.
15 H. Liu, G. Gaza-Bulseco, T. Xiang and C. Chumsae, *Mol. Immunol.*, 2008, **45**, 701–708.
16 L. Hou, I. Kang, R. E. Marchant and M. G. Zagorski, *J. Biol. Chem.*, 2002, **277**, 40173–40176.
17 L. Breydo, O. V. Bocharova, N. Makarava, V. V. Salnikov, M. Anderson and I. V. Baskakov, *Biochem*, 2005, **44**, 15534–15543.
18 S. D. Maleknia, N. Reixach and J. N. Buxbaum, *FEBS J.*, 2006, **273**, 5400–5406.
19 K. J. Binger, M. D. W. Griffin and G. J. Howlett, *Biochem*, 2008, **47**, 10208.
20 V. N. Uversky, G. Yamin, P. O. Souillac, J. Goers, C. B. Glaser and A. L. Fink, *FEBS Lett.*, 2002, **517**, 239–244.
21 G. Sancataldo, V. Vetri, V. Fodera, G. D. Cara, V. Militello and M. Leone, *PLOS ONE*, 2014, **9**, e84552.
22 Y. Q. Wong, K. J. Binger, G. Howlett and M. D. W. Griffin, *Proc. Natl. Acad. Sci. U. S. A.*, 2010, **107**, 1977–1982.
23 T. Koudelka, F. C. Dehle, I. F. Musgrave, P. Hoffmann and J. A. Carver, *J. Agric. Food Chem.*, 2012, **60**, 4144–4155.
24 N. Giamblanco, D. Coglitore, A. Gubbiotti, T. Ma, E. Balanzat, J. M. Janot, M. Chinappi and S. Balme, *Anal. Chem.*, 2018, **90**, 12900–12908.
25 S. Sardar, S. Pal, S. Maity, J. Chakraborty and U. C. Halder, *Int. J. Biol. Macromol.*, 2014, **69**, 137–145.
26 D. E. Dunstan, P. Hamilton-Brown, P. Asimakis, W. Duckera and J. Bertolini, *Soft Matter*, 2009, **5**, 5020–5028.
27 H. C. Liu, W. L. Chen and S. J. T. Mao, *J. Dairy Sci.*, 2007, **90**, 547–555.
28 J. Meltretter, C. M. Becker and M. Pischetsrieder, *J. Agric. Food Chem.*, 2008, **56**, 5165–5175.
29 R. G. Keck, *Anal. Biochem.*, 1996, **236**, 56–62.
30 J. Chakraborty, N. Das, K. P. Das and U. C. Halder, *Int. Dairy J.*, 2009, **19**, 43–49.
31 L. Zhou and R. J. Elias, *Food Chem.*, 2014, **146**, 521–530.
32 M. A. M. Hoffmann and P. J. J. M. vanMil, *J. Agric. Food Chem.*, 1999, **47**, 1898–1905.
33 R. N. Zuniga, A. Tolkach, U. Kulozik and J. M. Aguilera, *J. Food Sci.*, 2010, **75**, E261–E268.
34 M. R. Nilsson, *Methods*, 2004, **34**, 151–160.
35 G. V. Semisotnov, N. A. Radionava, O. I. Razgulyaev, V. N. Uversky, A. F. Gripas and R. I. Gilmanshin, *Biopolymer*, 1991, **31**, 119–128.
36 S. Sardar, Md. Anas, S. Maity, S. Pal, H. Parvej, S. Begum, R. Dalui, N. Sepay and U. C. Halder, *Int. J. Biol. Macromol.*, 2019, **125**, 596–604.
37 M. Behl, M. B. Kadiiska, M. R. Hejtmancik, D. Vasconcelos and R. S. Chhabra, *Cutaneous Ocul. Toxicol.*, 2012, **31**, 204–213.
38 Y. C. Yeh, T. J. Liu and H. C. Lai, *Int. J. Med. Sci.*, 2020, **4**(17), 368–382.
39 N. Fatemi, M. H. Sanati, M. Jamali Zavarehei, H. Ayat, V. Esmaeili, A. Golkar-Narenji, M. Zarabi and H. Gourabi, *Andrologia*, 2013, **45**(4), 232–239.
40 M. Boland, Whey proteins, Chemistry of beta-lactoglobulin, *Handbook of Food Proteins*, 2011, 3.3.1.
41 B. O. E. Mills, *Biochim. Biophys. Acta*, 1976, **434**, 324–332.
42 Y. Chen and M. D. Barkley, *Biochem*, 1998, **37**, 9976–9982.
43 S. Pal, S. Maity, S. Sardar, J. Chakraborty and U. C. Halder, *Int. J. Biol. Macromol.*, 2016, **84**, 121–134.
44 J. Ravi, A. E. Hills, E. Cerasoli, P. D. Rakowska and M. G. Ryadnov, *Eur. Biophys. J.*, 2011, **40**, 339–345.
45 S. Maity, S. Sardar, S. Pal, H. Parvej, J. Chakraborty and U. C. Halder, *RSC Adv.*, 2016, **6**, 74409–74417.
46 A. Barth, *Biochim. Biophys. Acta*, 2007, **1767**, 1073–1101.
47 V. Militello, V. Vetri and M. Leone, *Biophys. Chem.*, 2003, **105**, 133–141.
48 M. Collini, L. D'Alfonso and G. Baldini, *Protein Sci.*, 2000, **9**, 1968–1974.
49 L. D'Alfonso, M. Collini and G. Baldini, *Biochim. Biophys. Acta*, 1999, **1432**, 194–202.
50 G. Zolese, G. Falcioni, E. Bertoli, R. Galeazzi, M. Wozniak, Z. Wypych, E. Gratton and A. Ambrosini, *Proteins*, 2000, **40**, 39–48.
51 M. Collini, L. D'Alfonso, H. Molinari, L. Ragona, M. Catalano and G. Baldini, *Protein Sci.*, 2003, **12**, 1596–1603.
52 S. A. Hudson, H. Ecroyd, T. W. Kee and J. A. Carver, *FEBS J.*, 2009, **276**, 5960–5972.
53 J. D. Schmit, K. Ghosh and K. Dill, *Biophys. J.*, 2011, **100**, 450–458.
54 V. Fodera, A. Zaccone, M. Lattuada and A. M. Donald, *Phys. Rev. Lett.*, 2013, **111**, 108105.

55 J. C. Ioannou, A. M. Donald and R. H. Tromp, *Food Hydrocolloids*, 2015, **46**, 216–225.
56 R. Lumry and H. Eyring, *J. Phys. Chem.*, 1954, **58**, 110–120.
57 D. K. Chou, R. Krishnamurthy, M. C. Manning, T. W. Randolph and J. F. Carpenter, *J. Pharm. Sci.*, 2013, **102**, 660–673.
58 M. Anraku, K. Yamasaki, T. Maruyama, U. Kragh-Hansen and M. Otagiri, *Pharm. Res.*, 2001, **18**, 632–639.
59 S. Hermeling, H. Schellekens, C. Maas, M. Gebbink, D. I. A. Crommelin and W. Jiskoot, *J. Pharm. Sci.*, 2006, **95**, 1084–1096.
60 S. Pal, S. Maity, S. Sardar, H. Parvej, N. Das, J. Chakraborty and U. C. Halder, *RSC Adv.*, 2016, **6**, 111299–111307.
61 M. R. H. Krebs, G. L. Devlin and A. M. Donald, *Biophys. J.*, 2009, **96**, 5013–5019.
62 J. Otte, S. B. Lomholt, T. Halkier and K. B. Qvist, *J. Agric. Food Chem.*, 2000, **48**, 2443–2447.
63 A. Hung, M. D. Griffin, G. J. Howlett and I. Yarovsky, *Eur. Biophys. J.*, 2008, **38**, 99–110.
64 B. Feng, Z. Wang, T. Liu, R. Jin, S. Wang, W. Wang, G. Xiao and Z. Zhou, *Biochim. Biophys. Acta*, 2014, **1842**, 2345–2356.
65 T. C Fricke, F. Echtermeyer, J. Zielke, J. de la Roche, M. R Filipovic, S. Claverol, C. Herzog, M. Tominaga, R. A. Pumroy, V. Y. Moiseenkova-Bell, P. M Zygmunt, A. Leffler and M. J Eberhardt, *Proc. Natl. Acad. Sci. U. S. A.*, 2019, **26**, 24359–24365.
66 N. J Agrawal, A. Dykstra, J. Yang, H. Yue, X. Nguyen, C. Kolvenbach and N. Angell, *J. Pharm. Sci.*, 2018, **107**, 1282–1289.
67 S. Maity, S. Pal, S. Sardar, N. Sepay, H. Parvej, S. Begum, R. Dalui, N. Das, A. Pradhan and U. C. Halder, *New J. Chem.*, 2018, **42**, 19260–19271.
68 N. Sepay, C. Guha, S. Maity and A. K. Mallik, *Eur. J. Org. Chem.*, 2017, **2017**, 6013–6022.
69 M. Kuitunen, E. Savilahti and A. Sarnesto, *Allergy*, 1994, **49**, 354–360.
70 A. C Krämer, A. Torreggiani and M. J. Davies, *J. Agric. Food Chem.*, 2017, **29**(65), 10258–10269.
71 Y. Liao, R. Alvarado, B. Phinney and B. Lonnerdal, *J. Proteome Res.*, 2011, **10**, 1746–1754.
72 J. Meleltretter, C. M. Becker and M. Pischetsrieder, *J. Agric. Food Chem.*, 2008, **56**, 5165–5171.